

# Full-sky correlation functions for CMB experiments with asymmetric window functions

Kin-Wang Ng\*

*Institute of Physics & Institute of Astronomy and Astrophysics,  
Academia Sinica, Taipei, Taiwan 11529, R.O.C.*

(Dated: July 22, 2018)

## Abstract

We discuss full-sky convolution of the instrumental beam with the CMB sky signal in CMB single-dish and interferometry experiments, using the method [13] that the measured temperature and polarization anisotropies are defined globally on the group manifold of the three-dimensional rotation by means of Wigner D-functions. We re-derive the anisotropy and polarization correlation functions incorporated with asymmetric window functions, which are then explicitly calculated for a single-dish elliptical Gaussian beam and an interferometric Gaussian beam.

PACS numbers: 95.75.Hi, 95.75.Kk, 98.70.Vc, 98.80.-k

arXiv:astro-ph/0409007v2 16 Sep 2004

---

\*Electronic address: [nkw@phys.sinica.edu.tw](mailto:nkw@phys.sinica.edu.tw)

## I. INTRODUCTION

Since the detection of the large-angle temperature anisotropy of the cosmic microwave background (CMB) by the Cosmic Background Explorer (COBE) satellite [1], many CMB measurements have reported detections or upper limits of the CMB temperature anisotropy power spectrum  $C_{Tl}$  over a wide range of  $l$  [2]. Recently, the Wilkinson Microwave Anisotropy Probe (WMAP) [3] has measured the  $C_{Tl}$  in an unprecedented accuracy for  $l < 800$  and thus made a precise estimation of a number of cosmological parameters.

Polarization of the CMB contains a wealth of information about the early universe as well. It can cross-check the measured  $C_{Tl}$  and improve the accuracy in determining the cosmological parameters. A CMB polarization field can be decomposed into an electric-type  $E$  mode and a magnetic-type  $B$  mode [4]. Recently, the DASI instrument, a ground-based interferometric array with degree-scale resolution, has detected the CMB  $E$  polarization and  $TE$  cross-correlation, while setting an upper limit on the  $B$  polarization [5]. Furthermore, the WMAP has measured the  $TE$  power spectrum [6], which is consistent with theoretical predictions based on the measured CMB anisotropy and indicates a significant large-scale  $E$  polarization. Measuring the CMB polarization has become one of the main goals of CMB experiments [7]. Future ground-based and balloon-borne experiments and the Planck satellite will unveil detailed features of the CMB anisotropies, thus allowing one to determine to a high precision the cosmological parameters.

As high-resolution data made by high-sensitivity CMB experiments comes along, it will be necessary to consider the effect of beam asymmetry in data analysis in order to make unbiased estimation of the power spectra and ultimately of the cosmological parameters. This effect, mainly caused by the off-axis position of the detector in the focal plane of the telescope, is small and so far has been largely neglected in CMB data analysis. Recently, the effect of beam asymmetry has been investigated. Numerical studies [8, 9, 10, 11] have shown that the typical difference due to beam asymmetry is of few  $\mu K$  in Planck configuration and increases with the beamwidth and ellipticity [8] and that an azimuthally symmetrized beam does not bias the power spectrum estimates for most practical situations [9]. In Ref. [11], a fast convolution algorithm based on the decomposition of the asymmetric beam as a sum of circular Gaussian functions is developed. On the other hand, analytic methods have been formulated for treating arbitrary asymmetric beams in full-sky CMB temperature and polarization anisotropy experiments by using spin-weighted spherical harmonics [12] and Wigner D-functions [13]. In Ref. [13], the authors have pointed out that for asymmetric beam functions the result of convolutions is on the group manifold of the three-dimensional rotation and provided an algorithm for fast computation of the convolution on this group manifold. This method has been applied to study the effect of an elliptical Gaussian beam in the estimation of temperature and polarization correlation functions using semi-analytic or full numerical integration [14] and a perturbative series in powers of the ellipticity parameter [15].

In this paper, we will study the effect of beam asymmetry in full-sky CMB single-dish as well as interferometry experiments. We will derive the full-sky convolution for a complex asymmetric beam and define the measured temperature and polarization anisotropies globally on the group manifold of the three-dimensional rotation by using Wigner D-functions [13]. As such, we can extend the standard anisotropy and polarization correlation functions of domain over the celestial sphere to those over the rotation group manifold. The result is then applied to calculate the full-sky correlation functions for two typical cases: an elliptical Gaussian beam and an interferometric Gaussian beam. The former is a good

approximation to the actual shape of the window in most of CMB single-dish experiments and the latter is maximally asymmetric due to the finite length of the baseline of the interferometer. We will be able to obtain closed forms for the covariance matrices in both cases which are directly applicable in the CMB likelihood data analysis.

The paper is organized as follows. In Sec. II, a brief account of the building block of CMB anisotropies is given. We present the full-sky convolution of a complex asymmetric beam with the CMB sky in Sec. III. The full-sky CMB anisotropy and polarization correlation functions are re-derived in Sec. IV. In Sec. V, we apply the result to study the effect of beam asymmetry in two cases: a single-dish elliptical Gaussian beam and an interferometric Gaussian beam. The flat-sky limits of these two cases are discussed in Sec. VI. Sec. VII is our conclusions.

## II. CMB TEMPERATURE AND POLARIZATION ANISOTROPIES

Polarized emission is conventionally described in terms of the four Stokes parameters  $(I, Q, U, V)$ , where  $I$  is the intensity,  $Q$  and  $U$  represent the linear polarization, and  $V$  describes the circular polarization. Since circular polarization cannot be generated by Thomson scattering alone, the parameter  $V$  decouples from the other components and will not be considered. Let us define  $T$  be the temperature fluctuation about the mean; then, the CMB anisotropies are completely described by  $(T, Q, U)$ , where each parameter is a function of the pointing direction  $\hat{e}(\theta, \phi)$  on the celestial sphere.

Considering the CMB as Gaussian random fields, we can expand the Stokes parameters as [4]

$$\begin{aligned} T(\hat{e}) &= \sum_{lm} a_{0,lm} Y_{lm}(\hat{e}), \\ (Q - iU)(\hat{e}) &= \sum_{lm} a_{2,lm} {}_2Y_{lm}(\hat{e}), \\ (Q + iU)(\hat{e}) &= \sum_{lm} a_{-2,lm} {}_{-2}Y_{lm}(\hat{e}), \end{aligned} \quad (1)$$

where  $a_{0,lm}$  and  $a_{\pm 2,lm}$  are Gaussian random variables, and  ${}_{\pm 2}Y_{lm}$  are spin-2 spherical harmonics given by [16] [25]

$$\begin{aligned} {}_sY_{lm}(\theta, \phi) &= (-1)^{s+m} e^{im\phi} \left[ \frac{2l+1}{4\pi} \frac{(l+m)!}{(l+s)!} \frac{(l-m)!}{(l-s)!} \right]^{\frac{1}{2}} \sin^{2l} \left( \frac{\theta}{2} \right) \\ &\times \sum_r \binom{l-s}{r} \binom{l+s}{r+s-m} (-1)^{l-s-r} \cot^{2r+s-m} \left( \frac{\theta}{2} \right), \end{aligned} \quad (2)$$

where

$$\max(0, m-s) \leq r \leq \min(l-s, l+m). \quad (3)$$

Note that  ${}_sY_{lm}$  is related to Wigner D-functions  $D_{m'm}^l$  [17] by

$$D_{m'm}^l(\psi, \theta, \phi) = e^{-im'\psi} d_{m'm}^l(\theta) e^{-im\phi}, \quad \text{where} \quad {}_sY_{lm}(\theta, 0) = (-1)^{s+m} \sqrt{\frac{2l+1}{4\pi}} d_{-sm}^l(\theta). \quad (4)$$

It is straightforward to show the conjugation and symmetry relations

$${}_s Y_{lm}^*(\theta, \phi) = (-1)^{s+m} {}_{-s} Y_{l-m}(\theta, \phi), \quad (5)$$

$$D_{m'm}^l(\psi, \theta, \phi) = (-1)^{m'+m} D_{mm'}^l(\phi, \theta, \psi). \quad (6)$$

Isotropy in the mean guarantees the ensemble averages:

$$\begin{aligned} \langle a_{0,l'm'}^* a_{0,lm} \rangle &= C_{Tl} \delta_{l'l} \delta_{m'm}, \\ \langle a_{2,l'm'}^* a_{2,lm} \rangle &= (C_{El} + C_{Bl}) \delta_{l'l} \delta_{m'm}, \\ \langle a_{2,l'm'}^* a_{-2,lm} \rangle &= (C_{El} - C_{Bl}) \delta_{l'l} \delta_{m'm}, \\ \langle a_{0,l'm'}^* a_{2,lm} \rangle &= -C_{Cl} \delta_{l'l} \delta_{m'm}, \end{aligned} \quad (7)$$

where  $C_{Tl}$ ,  $C_{El}$ ,  $C_{Bl}$ , and  $C_{Cl}$  are respectively the anisotropy, E polarization, B polarization, and TE cross correlation angular power spectra.

Consider two pointings  $\hat{e}$  and  $\hat{e}'$  on the celestial sphere. By making use of Eq. (7) and the generalized addition theorem [12]

$$\sum_m {}_{s_1} Y_{lm}^*(\theta', \phi') {}_{s_2} Y_{lm}(\theta, \phi) = \sqrt{\frac{2l+1}{4\pi}} (-1)^{s_1-s_2} {}_{-s_1} Y_{ls_2}(\beta, \alpha) e^{-is_1\gamma}, \quad (8)$$

we find the two-point correlation functions [26]

$$\begin{aligned} \langle T^*(\hat{e}') T(\hat{e}) \rangle &= \sum_l \frac{2l+1}{4\pi} C_{Tl} P_l(\cos \beta), \\ \langle T^*(\hat{e}') [Q(\hat{e}) + iU(\hat{e})] \rangle &= - \sum_l \frac{2l+1}{4\pi} \sqrt{\frac{(l-2)!}{(l+2)!}} C_{Cl} P_l^2(\cos \beta) e^{-2i\alpha}, \\ \langle [Q(\hat{e}') + iU(\hat{e}')]^* [Q(\hat{e}) + iU(\hat{e})] \rangle &= \sum_l \sqrt{\frac{2l+1}{4\pi}} (C_{El} + C_{Bl}) {}_2Y_{l-2}(\beta, 0) e^{-2i(\alpha-\gamma)}, \\ \langle [Q(\hat{e}') - iU(\hat{e}')]^* [Q(\hat{e}) + iU(\hat{e})] \rangle &= \sum_l \sqrt{\frac{2l+1}{4\pi}} (C_{El} - C_{Bl}) {}_2Y_{l2}(\beta, 0) e^{-2i(\alpha+\gamma)}, \end{aligned} \quad (9)$$

where  $\beta$ ,  $\alpha$ , and  $\gamma$  are the angles defined in Fig. 1. Therefore, the statistics of the CMB anisotropy and polarization is fully described by the four independent power spectra or their corresponding correlation functions. The details about the evaluation of the power spectra can be found in Ref. [4].

### III. FULL-SKY COMPLEX ASYMMETRIC BEAM CONVOLUTION

In realistic CMB observations, as a result of the finite beam size of the antenna and the beam switching mechanism, a measurement is actually a convolution of the antenna response with the CMB Stokes parameters,

$$X_s^{\text{map}}(\hat{e}, \hat{u}) = \int d\hat{e}' R(\hat{e}'; \hat{e}, \hat{u}) X_s(\hat{e}'), \quad (10)$$

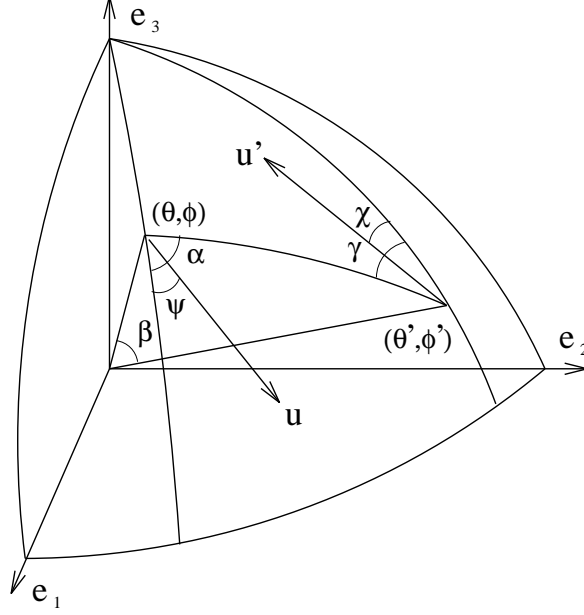


FIG. 1: Spherical coordinates showing two unit vectors  $\hat{e}'(\theta', \phi')$  and  $\hat{e}(\theta, \phi)$  with separation angle  $\beta$ . The angles between the great arc connecting the two points and the longitudes are  $\gamma$  and  $\alpha$ .  $\vec{u}$  is an arbitrary reference axis on the asymmetric beam pattern or an interferometric baseline vector tangential to the sphere with the orientation angle  $\psi$ .

where  $X_0 = T$ ,  $X_{\pm 2} = Q \mp iU$ , and  $R(\hat{e}'; \hat{e}, \hat{u})$  denotes the response function with the pointing direction  $\hat{e}$  and the orientation direction  $\hat{u}$  ( $\vec{u} = u\hat{u}$ , see Fig. 1). The orientation angle is denoted by  $\psi$  and therefore we have  $0 \leq \theta \leq \pi$ ,  $0 \leq \phi < 2\pi$ , and  $0 \leq \psi < 2\pi$ . Note that  $R(\hat{e}'; \hat{e}, \hat{u})$  may be an arbitrary complex function. Expanding

$${}_s Y_{lm}(\theta', \phi') = \sqrt{\frac{4\pi}{2l+1}} \sum_{m'} {}_s Y_{lm'}(\beta, \alpha) e^{is\gamma} {}_{-m'} Y_{lm}(\theta, \phi) \quad (11)$$

in Eq. (1), we obtain the full-sky convolution for an arbitrary beam function as [12]

$$X_s^{\text{map}}(\theta, \phi, \psi) = \sum_{lm} a_{s,lm} {}_{-m} Y_{lm}(\theta, \phi) \sqrt{\frac{4\pi}{2l+1}} \int \sin \beta d\beta d\alpha R(\beta, \alpha, \psi) {}_s Y_{lm'}(\beta, \alpha) e^{is\gamma}. \quad (12)$$

In typical CMB measurements, the field of view is small such that we can make a *local* flat-sky approximation  $\alpha = \gamma$ . After changing the integration variable  $\alpha \rightarrow \alpha - \psi$  in Eq. (12) and using Eq. (6), the orientation angle  $\psi$  of the response function is absorbed in the new variable and we thus obtain

$$X_s^{\text{map}}(\theta, \phi, \psi) = e^{is\psi} \sum_{lm} a_{s,lm} D_{mm'}^{l*}(\phi, \theta, \psi) \sqrt{\frac{2l+1}{4\pi}} {}_s b_{lm'}, \quad (13)$$

$${}_s b_{lm'} = \sqrt{\frac{4\pi}{2l+1}} \int \sin \beta d\beta d\alpha R(\beta, \alpha) {}_s Y_{lm'}(\beta, \alpha) e^{is\alpha}.$$

This equation was first derived in Ref. [13] by using an alternative way. From the conjugation relation (5), we have  ${}_s b_{lm}^* = (-1)^{s+m} {}_{-s} b_{l-m}$ . We define a spin- $s$  window function

$${}_s W_l \equiv \sum_m |{}_s b_{lm}|^2. \quad (14)$$

For a simple single-dish experiment with an axisymmetric Gaussian response function given by

$$R^G(\beta, \alpha) = \frac{1}{2\pi\sigma_b^2} \exp\left(-\frac{\beta^2}{2\sigma_b^2}\right), \quad (15)$$

where  $\sigma_b \ll 1$  is the Gaussian beamwidth, it can be shown from Eq. (13) that [12, 13]

$${}_s b_{lm}^G = {}_s W_l^{G\frac{1}{2}} \delta_{-m,s}, \quad (16)$$

$$X_s^{\text{map}}(\theta, \phi) = \sum_{lm} a_{s,lm} {}_s W_l^{G\frac{1}{2}} {}_s Y_{lm}(\theta, \phi), \quad (17)$$

$$\text{where } {}_s W_l^G = \exp\left\{-\left[l(l+1) - s^2\right]\sigma_b^2\right\}. \quad (18)$$

For  $s = 0, \pm 2$  and  $\sigma_b \rightarrow 0$ , the Gaussian window function  ${}_s W_l^G \rightarrow 1$  and Eq. (17) reduces to Eq. (1).

#### IV. CORRELATION FUNCTIONS ON ROTATION GROUP MANIFOLD

The result in Eq. (13) shows that CMB measurements with asymmetric beam, although the sky is approximated as flat locally, can be interconnected globally on the celestial sphere extended with a circle space of the orientation angle of the asymmetric beam. More precisely, the observed anisotropies are well-defined on the group manifold of the three-dimensional rotation [13]. Let us denote a point on the manifold by  $\vec{r} = (\hat{e}, \hat{u}) = (\theta, \phi, \psi)$ , then by making use of Eqs. (7), (8), and (13), we obtain the two-point correlation functions (see also Refs. [14, 15])

$$\begin{aligned} \langle X_{s'}^{\text{map}*}(\vec{r}') X_s^{\text{map}}(\vec{r}) \rangle = & e^{-is'\psi'} e^{is\psi} \sum_{lm'm} \sqrt{\frac{2l+1}{4\pi}} C_{s's,l} (-1)^{m'+m} {}_{m'} Y_{l-m}(\beta, 0) \times \\ & e^{-im(\alpha-\psi)} e^{im'(\gamma-\psi')} {}_{s'} b_{lm'}^* {}_s b_{lm}, \end{aligned} \quad (19)$$

where  $C_{00,l} = C_{T,l}$ ,  $C_{0-2,l} = -C_{C,l}$ , and  $C_{\mp 2-2,l} = C_{E,l} \pm C_{B,l}$ . For a Gaussian beam given in Eq. (15), substituting the result from Eq. (16) for both  ${}_s b_{lm}$  and  ${}_{s'} b_{lm'}$  in Eq. (19), we obtain

$$\langle X_{s'}^{\text{map}*}(\vec{r}') X_s^{\text{map}}(\vec{r}) \rangle = \sum_l \sqrt{\frac{2l+1}{4\pi}} C_{s's,l} {}_{-s'} Y_{ls}(\beta, 0) e^{is\alpha} e^{-is'\gamma} {}_{s'} W_l^{G\frac{1}{2}} {}_s W_l^{G\frac{1}{2}}, \quad (20)$$

where  ${}_s W_l^G$  is the Gaussian window function given in Eq. (18). This reduces to the correlation functions in Eq. (9) as the Gaussian beamwidth  $\sigma_b \rightarrow 0$ .

To write Eq. (19) in a compact form, we define  $\bar{X}_s^{\text{map}}(\vec{r}) = e^{-is\psi} X_s^{\text{map}}(\vec{r})$ ,  $\bar{\alpha} = \alpha - \psi$ , and  $\bar{\gamma} = \gamma - \psi$  where  $\psi' = \pi + \chi$ . After using Eq. (4), we obtain

$$\langle \bar{X}_{s'}^{\text{map}*}(\vec{r}') \bar{X}_s^{\text{map}}(\vec{r}) \rangle = \sum_{lm'm} \frac{2l+1}{4\pi} C_{s's,l} (-1)^{m'} D_{mm'}^l(\bar{\alpha}, \beta, -\bar{\gamma}) {}_{s'} b_{lm'}^* {}_s b_{lm}. \quad (21)$$

Note that  $\bar{\alpha}$  and  $\bar{\gamma}$  are respectively the angles between the orientation directions at the pointings  $\hat{e}$  and  $\hat{e}'$  and the great arc connecting the two pointing directions (see Fig. 1). Furthermore, the root-mean-square anisotropy and polarization fluctuations are given by

the correlation functions (21) at zero lag. By taking  $\vec{r}' \rightarrow \vec{r}$  and making use of the limiting property (Eq. (4.16.2) of Ref. [17])

$$D_{mm'}^l(\alpha, 0, \gamma) = \delta_{mm'} e^{-im(\alpha+\gamma)}, \quad (22)$$

we have  $\bar{\alpha} - \bar{\gamma} = -\pi$  and

$$\langle |X_s^{\text{map}}(\vec{r})|^2 \rangle = \sum_l \frac{2l+1}{4\pi} C_{ss,l} {}_sW_l, \quad (23)$$

where  ${}_sW_l$  is given by Eq. (14).

Eq. (21) is useful for constructing the covariance matrices in the likelihood analysis of CMB data made by an asymmetric beam. In the next section, we will show that in most practical cases the summation in Eq. (21) can be largely reduced to a tractable one. For examples, in the case of a slightly elliptical Gaussian beam, the summation over  $m$  for a fixed  $l$  converges very fast as  $|{}_sb_{lm}|/|{}_sb_{l0}|$  falls off rapidly with increasing  $|m|$ . In the case of an interferometric beam with a long baseline  $|{}_sb_{lm}|$  is approximately dependent on  $l$  only.

## V. ASYMMETRIC WINDOW FUNCTIONS: TWO CASES

In deriving the main result (13), we have approximated the sky as locally flat. This is a good approximation for CMB experiments with high spatial resolution or small fields of view. We can further evaluate the integral for  ${}_sb_{lm}$  in Eq. (13) by use of the approximation (Eq. (4.18.1.2) of Ref. [17]),

$$d_{-sm}^l(\theta) \simeq (-1)^{s+m} J_{s+m}(l\theta) \quad \text{for } l \gg 1, \quad (24)$$

where  $J_n(x)$  are Bessel functions and we have used the property  $J_{-n}(x) = (-1)^n J_n(x)$ . Below we discuss two typical cases in CMB experiments.

### A. Single-dish Elliptical Gaussian Beam

For most of simple CMB single-dish experiments, the response function can be approximated by an elliptical Gaussian beam,

$$R^{EG}(\beta, \alpha) = \frac{1}{2\pi\sigma_x\sigma_y} \exp\left(-\frac{x^2}{2\sigma_x^2} - \frac{y^2}{2\sigma_y^2}\right), \quad (25)$$

where  $x = \beta \cos \alpha$ ,  $y = \beta \sin \alpha$ , and  $\sigma_x$  and  $\sigma_y$  are the beamwidths in the major and minor axes respectively. Here we assume  $\sigma_x \ll 1$  and  $\sigma_y \ll 1$ . Substituting the beam (25) in Eq. (13), making the approximation (24) in the integral, and using Eqs. (3.915.2) and (6.651.6) of Ref. [18] to perform the  $\alpha$ -integration and  $\beta$ -integration respectively, we obtain

$${}_sb_{lm}^{EG} \simeq \frac{1}{2} [1 + (-1)^{s+m}] \exp[-l^2(\sigma_x^2 + \sigma_y^2)/4] I_{(s+m)/2}(l^2(\sigma_x^2 - \sigma_y^2)/4) \\ \text{for } s+m > -1 \quad \text{and} \quad 1 > (\sigma_x^2 - \sigma_y^2)/\sigma_x^2, \quad (26)$$

where  $I_n(x)$  are modified Bessel functions. For  $s = 0$ , the result coincides with that for an unpolarized elliptical Gaussian beam found in Ref. [19]. In the limit of  $\sigma_x \rightarrow \sigma_y$ , since

$I_{(s+m)/2}(0) = \delta_{-m,s}$ , we obtain that  ${}_s b_{lm}^{EG} \simeq \exp(-l^2 \sigma_y^2/2) \delta_{-m,s}$ . This is expected for an Gaussian beam as discussed in Eq. (16). From Eq. (26), the elliptical Gaussian window function is given by

$${}_0 W_l^{EG} \simeq \exp \left[ -l^2 (\sigma_x^2 + \sigma_y^2)/2 \right] \left[ I_0^2(z) + 2 \sum_{n=1}^{\lfloor l/2 \rfloor} I_n^2(z) \right], \quad (27)$$

$${}_{\pm 2} W_l^{EG} \simeq \exp \left[ -l^2 (\sigma_x^2 + \sigma_y^2)/2 \right] \left[ I_0^2(z) + 2 \sum_{n=1}^{\lfloor l/2 \rfloor - 1} I_n^2(z) + I_{\lfloor l/2 \rfloor}^2(z) + I_{\lfloor l/2 \rfloor + 1}^2(z) \right], \quad (28)$$

where  $z = l^2(\sigma_x^2 - \sigma_y^2)/4$  and  $\lfloor l/2 \rfloor$  denotes the integer part of  $l/2$ . Making use of the relation (Eq. (8.537.2) of Ref. [18])

$$\sum_{k=-\infty}^{\infty} J_k(z) J_{n-k}(z) = J_n(2z) \quad \text{and} \quad I_k(z) = i^{-k} J_k(iz), \quad (29)$$

we find that for  $z < 1$ ,

$${}_s W_l^{EG} \simeq \exp \left[ -l^2 (\sigma_x^2 + \sigma_y^2)/2 \right] I_0 \left( l^2 (\sigma_x^2 - \sigma_y^2)/2 \right). \quad (30)$$

## B. Interferometric Gaussian Beam

Recent advancement in low-noise, broadband, GHz amplifiers has made interferometry a particularly attractive technique for detecting CMB anisotropies. An interferometric array is intrinsically a high-resolution polarimetric instrument, well suited to observing small-scale polarized intensity fluctuations while being flexible in the coverage of a wide range of angular scales, with resolution and sensitivity determined by the aperture of each element of the array and the baselines formed by the array elements. In addition, many systematic problems inherent in single-dish experiments, such as ground and near field atmospheric pickup, and spurious polarization signal, can be reduced or avoided in interferometry. Being ground-based, it is controllable, and it can track the sky for an extensive period of time, as practiced successfully by the DASI team in measuring the CMB  $E$  polarization [5]. Observational strategies of CMB interferometry experiments such as DASI, CBI, VSA, and AMiBA can be found in Ref. [20] and references therein.

In contrast to single-dish experiments which measure or differentiate the signals in individual dishes, an interferometer measures the correlation of the signals from different pairs of the array elements. The correlation output is called the complex visibility. In typical interferometric measurements, the field of view is small so that the sky can be treated as flat. Therefore, the complex visibility is simply the two-dimensional Fourier transform of the intensity fluctuations on the sky convolved with the primary beam of the interferometer. The capability of directly sampling the Fourier modes allows for a simple estimation of the anisotropy power spectrum from visibility data [21] and an efficient separation of the  $E$  and  $B$  polarization power spectra [22]. However, as the sky coverage is increased in mosaicking observations which combine several contiguous pointings of the telescope, the curvature of the sky becomes significant even though the sky is locally flat at each pointing. Here we apply the results in the previous sections to extend the flat-sky formalism of the complex



visibility to including the curvature effect of the sky. For further discussions about large-angular-scale interferometry in which three-dimensional Fourier transforms are involved, the reader may refer to Ref. [23].

Let us consider a two-element interferometer and a monochromatic electromagnetic source. The complex visibility is the time-averaged correlation of the electric field measured by the two separated antennae pointing in the same direction to the sky [24]. Usually, each antenna has a pair of feeds which are sensitive to orthogonal circular or linear polarizations. For instance, if the dual-polarization feeds measure the right and left circular polarizations, then the output will be the four correlations  $\langle RR^* \rangle$ ,  $\langle RL^* \rangle$ ,  $\langle LR^* \rangle$ , and  $\langle LL^* \rangle$ . They can be related to Stokes parameters  $(T, Q, U, V)$ . Denoting their associated visibility functions by  $(V_T, V_Q, V_U, V_V)$ , we have

$$\begin{aligned}\langle RR^* \rangle &= V_T + V_V, \\ \langle LL^* \rangle &= V_T - V_V, \\ \langle RL^* \rangle &= V_Q + iV_U \equiv V_{-2}, \\ \langle LR^* \rangle &= V_Q - iV_U \equiv V_{+2},\end{aligned}\tag{31}$$

where we have neglected the parallactic angle of the feed with respect to the sky and the leakage from one polarization channel to the other polarization channel. The visibility functions are given by

$$V_s(\hat{e}, \vec{u}) = \frac{\partial B_\nu}{\partial T} \int d\hat{e}' A(\hat{e}'; \hat{e}) X_s(\hat{e}') e^{2\pi i \vec{u} \cdot \hat{e}'},\tag{32}$$

where  $\vec{u}$  is the separation vector (baseline) of the two antennae measured in units of the observation wavelength,  $A$  denotes the primary beam with the phase tracking center pointing along the direction  $\hat{e}$ , and  $X_s$  is the CMB sky. In Eq. (32),  $\partial B_\nu / \partial T$  is a conversion factor from the CMB temperature fluctuation to the brightness fluctuation given by

$$\frac{\partial B_\nu}{\partial T} \simeq 99.27 \frac{x^4 e^x}{(e^x - 1)^2} \text{Jy sr}^{-1} \mu\text{K}^{-1}, \quad \text{where } x \simeq 1.76 \left( \frac{\nu}{100\text{GHz}} \right),\tag{33}$$

where  $B_\nu$  is the Planck function of the photon frequency  $\nu$ .

Therefore, the response function of the interferometer is a complex function

$$R^I(\hat{e}'; \hat{e}, \vec{u}) = A(\hat{e}'; \hat{e}) e^{2\pi i \vec{u} \cdot \hat{e}'}. \tag{34}$$

Usually, the observation wavelength is much smaller than the size of the primary beam, dictating a small field of view. As such, for a single pointing, we can make the flat-sky approximation by decomposing

$$\hat{e}' = \hat{e} + \vec{\beta}, \quad \text{with } \vec{\beta} \cdot \hat{e} = 0, \quad \text{and } |\vec{\beta}| \ll 1. \tag{35}$$

Here we assume a Gaussian primary beam given by

$$A(\beta, \alpha) = \exp\left(-\frac{\beta^2}{2\sigma_b^2}\right). \tag{36}$$

Hence, by writing  $\vec{u} \cdot \hat{e}' = \vec{u} \cdot \vec{\beta} = u\beta \cos \alpha$  in Eq. (34), the interferometric response function becomes

$$R^{IG}(\beta, \alpha) = A(\beta, \alpha) e^{i2\pi u \beta \cos \alpha}. \tag{37}$$

Note that in Eq. (36) we have adopted the interferometry convention that the primary beam does not carry the normalization factor  $1/(2\pi\sigma_b^2)$ . Moreover, we have assumed a symmetric primary beam because a small beam asymmetry introduces only higher-order corrections which can be neglected as long as the length of the baseline is much bigger than the size of the dish.

Similar to the previous case, substituting the beam (37) in Eq. (13), making the approximation (24) in the integral, and using Eqs. (3.915.2) and (6.633.2) of Ref. [18] to perform the  $\alpha$ -integration and  $\beta$ -integration respectively, we obtain

$${}_s b_{lm}^{IG} \simeq i^{s+m} 2\pi\sigma_b^2 \exp\left[-\sigma_b^2(l^2 + l_u^2)/2\right] I_{s+m}(ll_u\sigma_b^2), \quad (38)$$

where  $l_u = 2\pi u$  is the peak location of the primary beam. When the baseline length is much bigger than the antenna size, we have the limiting form

$$I_{s+m}(ll_u\sigma_b^2) \simeq e^{ll_u\sigma_b^2}/\sqrt{2\pi ll_u\sigma_b^2} \quad \text{for } ll_u\sigma_b^2 \gg 1. \quad (39)$$

Therefore, for long baselines, Eq. (38) can be approximated as

$${}_s b_{lm}^{IG} \simeq i^{s+m} \sqrt{\frac{2\pi\sigma_b^2}{ll_u}} \exp\left[-\sigma_b^2(l - l_u)^2/2\right], \quad (40)$$

which is actually a Gaussian beam centered at  $l = l_u = 2\pi u$ . From Eq. (38), the interferometric Gaussian window function is given by

$${}_0 W_l^{IG} \simeq 4\pi^2\sigma_b^4 \exp\left[-\sigma_b^2(l^2 + l_u^2)\right] \left[ I_0^2(z) + 2 \sum_{n=1}^l I_n^2(z) \right], \quad (41)$$

$${}_{\pm 2} W_l^{IG} \simeq 4\pi^2\sigma_b^4 \exp\left[-\sigma_b^2(l^2 + l_u^2)\right] \left[ I_0^2(z) + 2 \sum_{n=1}^{l-2} I_n^2(z) + \sum_{n=l-1}^{l+2} I_n^2(z) \right], \quad (42)$$

where  $z = ll_u\sigma_b^2$ . Again, making use of Eq. (29), we find that for  $z < 1$ ,

$${}_s W_l^{IG} \simeq 4\pi^2\sigma_b^4 \exp\left[-\sigma_b^2(l^2 + l_u^2)\right] I_0(2ll_u\sigma_b^2). \quad (43)$$

## VI. FLAT-SKY APPROXIMATION

We have discussed the full-sky CMB temperature and polarization correlation functions for asymmetric small-scale beams. In the limit of small sky coverage, their limiting forms must coincide with the results that are obtained in the flat-sky approximation. In this limit, the sky can be treated as flat, being spanned by a two-dimensional vector  $\mathbf{r}$ . Hence, the CMB anisotropy and polarization fields are given by the Fourier transforms

$$\begin{aligned} T(\mathbf{r}) &= \int d\mathbf{u} \tilde{T}(\mathbf{u}) e^{-2\pi i \mathbf{u} \cdot \mathbf{r}}, \\ Q(\mathbf{r}) \pm iU(\mathbf{r}) &= \int d\mathbf{u} \left[ \tilde{E}(\mathbf{u}) \mp i\tilde{B}(\mathbf{u}) \right] e^{\mp i 2\phi_{\mathbf{u}}} e^{-2\pi i \mathbf{u} \cdot \mathbf{r}}, \end{aligned} \quad (44)$$

where  $\phi_{\mathbf{u}}$  is the phase in the Fourier space given by the direction angle of  $\mathbf{u}$  and

$$\begin{aligned} \langle \tilde{Y}^*(\mathbf{u}) \tilde{Y}(\mathbf{w}) \rangle &= S_{YY}(u) \delta(\mathbf{u} - \mathbf{w}) \quad \text{where } Y = T, E, B, \\ \langle \tilde{T}^*(\mathbf{u}) \tilde{E}(\mathbf{w}) \rangle &= S_{TE}(u) \delta(\mathbf{u} - \mathbf{w}). \end{aligned} \quad (45)$$

The power spectrum  $S(u)$  defined in the  $\mathbf{u}$ -plane can be related to the angular power spectrum  $C_l$  defined on the sphere by  $l(l+1)C_l/2\pi \simeq 2\pi u^2 S(u)$ , with  $l \simeq 2\pi u$ .

### A. Single-dish Elliptical Gaussian Beam

With an elliptical Gaussian beam with orientation angle  $\psi$  given by

$$R^{EG}(\mathbf{r}, \psi) = \frac{1}{2\pi\sigma_x\sigma_y} \exp \left[ -\frac{r^2 \cos^2(\theta - \psi)}{2\sigma_x^2} - \frac{r^2 \sin^2(\theta - \psi)}{2\sigma_y^2} \right], \quad (46)$$

where  $\mathbf{r} = (r \cos \theta, r \sin \theta)$ , the single-dish measurement gives

$$X_s^{\text{map}}(\mathbf{r}, \psi) = \int d\mathbf{r}' R^{EG}(\mathbf{r}' - \mathbf{r}, \psi) X_s(\mathbf{r}'), \quad (47)$$

where  $X_0 = T$ ,  $X_{\pm 2} = Q \mp iU$ , and  $\mathbf{r}$  is a pointing position on the sky. Using the expansion (44) and the Fourier transform of the response function

$$R^{EG}(\mathbf{r}, \psi) = \int d\mathbf{u} \tilde{R}^{EG}(\mathbf{u}, \psi) e^{-2\pi i \mathbf{u} \cdot \mathbf{r}}, \quad (48)$$

the measured anisotropies can be written as

$$X_s^{\text{map}}(\mathbf{r}, \psi) = \int d\mathbf{w} \tilde{R}^{EG}(-\mathbf{w}, \psi) \tilde{X}_s(\mathbf{w}) e^{is\phi_{\mathbf{w}}} e^{-2\pi i \mathbf{w} \cdot \mathbf{r}}, \quad (49)$$

where  $\tilde{X}_0 = \tilde{T}$  and  $\tilde{X}_{\pm 2} = \tilde{E} \pm i\tilde{B}$ . Hence, using Eq. (45) the two-point correlation function with different orientation angles at each point is given by

$$\begin{aligned} & \langle X_{s'}^{\text{map}*}(\mathbf{r}', \psi') X_s^{\text{map}}(\mathbf{r}, \psi) \rangle \\ &= \int dw w S_{s's}(w) \int \phi_{\mathbf{w}} e^{-i(s'-s)\phi_{\mathbf{w}}} e^{-2\pi i w |\mathbf{r}' - \mathbf{r}| \cos \phi_{\mathbf{w}}} \tilde{R}^{EG*}(-\mathbf{w}, \psi') \tilde{R}^{EG}(-\mathbf{w}, \psi), \end{aligned} \quad (50)$$

where  $S_{00} = S_{TT}$ ,  $S_{\pm 2 \pm 2} = S_{EE} + S_{BB}$ ,  $S_{\pm 2 \mp 2} = S_{EE} - S_{BB}$ ,  $S_{0 \pm 2} = S_{TE}$ , and  $\phi_{\mathbf{w}}$  is the angle between  $\mathbf{r} - \mathbf{r}'$  and  $\mathbf{w}$ . Expanding (see Eq. (8.511.4) of Ref. [18])

$$e^{-2\pi i w |\mathbf{r}' - \mathbf{r}| \cos \phi_{\mathbf{w}}} = \sum_{m=-\infty}^{\infty} (-i)^m J_m(2\pi w |\mathbf{r}' - \mathbf{r}|) e^{-im\phi_{\mathbf{w}}} \quad (51)$$

and using Eq. (3.915.2) of Ref. [18] to perform the  $\phi$ -integration, we finally obtain

$$\begin{aligned} & \langle X_{s'}^{\text{map}*}(\mathbf{r}', \psi') X_s^{\text{map}}(\mathbf{r}, \psi) \rangle \\ &= \int dw w S_{s's}(w) \exp \left[ -2\pi^2 w^2 (\sigma_x^2 + \sigma_y^2) \right] \sum_{m=-\infty}^{\infty} \pi \left[ (-1)^{s'-s} + (-1)^m \right] e^{-i(s'-s+m)(\psi'+\psi)/2} \times \\ & \quad i^m J_m(2\pi w |\mathbf{r}' - \mathbf{r}|) I_{(s'-s+m)/2} \left( 2\pi^2 w^2 (\sigma_y^2 - \sigma_x^2) \cos(\psi' - \psi) \right). \end{aligned} \quad (52)$$

At zero lag, the non-vanishing contribution is from  $m = 0$  since  $J_m(0) = \delta_{m,0}$  and thus

$$\langle |X_s^{\text{map}}(\mathbf{r}, \psi)|^2 \rangle = \int dw w S_{ss}(w) \exp \left[ -2\pi^2 w^2 (\sigma_x^2 + \sigma_y^2) \right] 2\pi I_0 \left( 2\pi^2 w^2 (\sigma_y^2 - \sigma_x^2) \right), \quad (53)$$

which reproduces the result as found in Eq. (23), with the window function given by Eq. (30) and the replacement  $l = 2\pi w$ . By taking the limit  $\sigma_x \rightarrow \sigma_y$  and using  $I_{(s'-s+m)/2}(0) = \delta_{-m, s'-s}$ , we obtain the standard two-point correlation functions with a Gaussian window

$$\langle X_{s'}^{\text{map}*}(\mathbf{r}') X_s^{\text{map}}(\mathbf{r}) \rangle = \int dw w S_{s's}(w) \exp \left( -4\pi^2 w^2 \sigma_y^2 \right) 2\pi (-i)^{s'-s} J_{s'-s}(2\pi w |\mathbf{r}' - \mathbf{r}|). \quad (54)$$

## B. Interferometric Gaussian Beam

In the flat-sky approximation (35), the complex visibility (32) is reduced to the two-dimensional Fourier transform of the Stokes parameter multiplied by the primary beam,

$$V_s(\mathbf{r}, \mathbf{u}) = \frac{\partial B_\nu}{\partial T} \int d\mathbf{r}' A(\mathbf{r}' - \mathbf{r}) X_s(\mathbf{r}') e^{2\pi i \mathbf{u} \cdot \mathbf{r}'}, \quad (55)$$

where  $\mathbf{u}$  is the two-dimensional projection vector of the baseline between two dishes in the  $\mathbf{r}$ -plane and  $\mathbf{r}$  is a pointing position on the sky. Therefore, we have

$$V_s(\mathbf{r}, \mathbf{u}) = \frac{\partial B_\nu}{\partial T} e^{2\pi i \mathbf{u} \cdot \mathbf{r}} \int d\mathbf{w} \tilde{A}(\mathbf{u} - \mathbf{w}) \tilde{X}_s(\mathbf{w}) e^{i s \phi_{\mathbf{w}}} e^{-2\pi i \mathbf{w} \cdot \mathbf{r}}. \quad (56)$$

Hence, the two-point correlation function with different baselines at each point is given by

$$\begin{aligned} \langle V_{s'}^*(\mathbf{r}', \mathbf{u}') V_s(\mathbf{r}, \mathbf{u}) \rangle &= \left( \frac{\partial B_\nu}{\partial T} \right)^2 e^{-2\pi i (\mathbf{u}' \cdot \mathbf{r}' - \mathbf{u} \cdot \mathbf{r})} \int dw w S_{s's}(w) \times \\ &\int \phi_{\mathbf{w}} e^{-i(s'-s)\phi_{\mathbf{w}}} e^{-2\pi i w |\mathbf{r}' - \mathbf{r}| \cos \phi_{\mathbf{w}}} \tilde{A}^*(\mathbf{u}' - \mathbf{w}) \tilde{A}(\mathbf{u} - \mathbf{w}). \end{aligned} \quad (57)$$

Assuming a Gaussian primary beam (36) and using Eqs. (3.937.1) and (3.937.2) of Ref. [18] to perform the  $\phi$ -integration, we obtain for  $s' \geq s$

$$\begin{aligned} \langle V_{s'}^*(\mathbf{r}', \mathbf{u}') V_s(\mathbf{r}, \mathbf{u}) \rangle &= \left( \frac{\partial B_\nu}{\partial T} \right)^2 e^{-2\pi i (\mathbf{u}' \cdot \mathbf{r}' - \mathbf{u} \cdot \mathbf{r})} \int dw w S_{s's}(w) \exp \left[ -2\pi^2 \sigma_b^2 (u'^2 + u^2 + 2w^2) \right] \times \\ &8\pi^3 \sigma_b^4 \left[ \frac{(p + iq)^2 + a^2}{p^2 + (a + q)^2} \right]^{(s'-s)/2} I_{s'-s} \left( \sqrt{(p + ia)^2 + q^2} \right), \end{aligned} \quad (58)$$

where

$$\begin{aligned} a &= 2\pi w |\mathbf{r}' - \mathbf{r}|, \\ p &= 4\pi^2 \sigma_b^2 w (u' \cos \phi_{\mathbf{u}'} + u \cos \phi_{\mathbf{u}}), \\ q &= -4\pi^2 \sigma_b^2 w (u' \sin \phi_{\mathbf{u}'} + u \sin \phi_{\mathbf{u}}). \end{aligned} \quad (59)$$

As  $|\mathbf{r}' - \mathbf{r}| \rightarrow 0$  and we set  $\mathbf{r} = \mathbf{0}$  without loss of generality, we obtain the single-pointing visibility covariance matrices

$$\begin{aligned} \langle V_{s'}^*(\mathbf{u}') V_s(\mathbf{u}) \rangle &= \left( \frac{\partial B_\nu}{\partial T} \right)^2 \int dw w S_{s's}(w) \exp \left[ -2\pi^2 \sigma_b^2 (u'^2 + u^2 + 2w^2) \right] \times \\ &8\pi^3 \sigma_b^4 e^{-i(s'-s)\phi_U} I_{s'-s} \left( 4\pi^2 \sigma_b^2 w |U| \right), \end{aligned} \quad (60)$$

where  $U = |U| e^{i\phi_U} = u' e^{i\phi_{\mathbf{u}'}} + u e^{i\phi_{\mathbf{u}}}$ , explicitly given by

$$\begin{aligned} |U| &= [u'^2 + u^2 + 2u'u \cos(\phi_{\mathbf{u}'} - \phi_{\mathbf{u}})]^{\frac{1}{2}}, \\ \phi_U &= \tan^{-1} [(u' \sin \phi_{\mathbf{u}'} + u \sin \phi_{\mathbf{u}}) / (u' \cos \phi_{\mathbf{u}'} + u \cos \phi_{\mathbf{u}})]. \end{aligned} \quad (61)$$

In a special case when  $|\mathbf{u}'| = |\mathbf{u}| = u$ , we have  $|U| = 2u |\cos[(\phi_{\mathbf{u}'} - \phi_{\mathbf{u}})/2]|$  and  $\phi_U = (\phi_{\mathbf{u}'} + \phi_{\mathbf{u}})/2$ . Finally, the root-mean-square visibility is given by

$$\langle |V_s(\mathbf{r}, \mathbf{u})|^2 \rangle = \left( \frac{\partial B_\nu}{\partial T} \right)^2 8\pi^3 \sigma_b^4 \int dw w S_{ss}(w) \exp \left[ -4\pi^2 \sigma_b^2 (u^2 + w^2) \right] I_0(8\pi^2 \sigma_b^2 u w), \quad (62)$$

which reproduces the result as found in Eq. (23), with the window function given by Eq. (43) and the replacement  $l = 2\pi w$ .

## VII. CONCLUSIONS

Next-generation CMB experiments with high resolution and sensitivity will need to take into account the effect of beam asymmetry in interpreting observational data, while the pipeline for data analysis in CMB interferometric measurements using the flat-sky approximation will have to be modified to including the effect of the sky curvature to deal with future observational data with large sky coverage. We have thus studied full-sky CMB anisotropy and polarization measurements with asymmetric beams. The measured Stokes parameters are well defined globally on the group manifold of the three-dimensional rotation and we have derived their correlation functions on the group manifold. The correlation functions are useful for constructing the full covariance matrices in the maximum-likelihood data analysis in large-sky CMB experiments with asymmetric window functions, especially when the beam is highly asymmetric and it is difficult to do beam symmetrization. Moreover, the domain of the CMB observable field is extended from the celestial sphere on which the field is expanded in terms of spherical harmonics to the rotation group manifold on which the field is expanded in terms of Wigner D-functions. As such, unbiased CMB angular anisotropy and polarization power spectra can be directly deconvoluted from observational data by converting the Wigner D-functions on the rotation group manifold. Work along this line is in progress.

### Acknowledgments

The author would like to thank the Berkeley Cosmology Group for their useful discussions and hospitality during his visit, where part of the work has been done. This work was supported in part by the National Science Council, ROC under the Grant NSC93-2112-M-001-013.

- 
- [1] G. F. Smoot *et al.*, *Astrophys. J.* **369**, L1 (1992).
  - [2] For reviews, see F. R. Bouchet as well as A. H. Jaffe, *Proceedings of the 2002 International Symposium in Cosmology and Particle Astrophysics*, Taiwan, edited by X.-G. He *et al.* (World Scientific, Singapore, 2003).
  - [3] C. L. Bennett *et al.*, *Astrophys. J. Suppl.* **148**, 1 (2003).
  - [4] M. Zaldarriaga and U. Seljak, *Phys. Rev. D* **55**, 1830 (1997); M. Kamionkowski, A. Kosowsky, and A. Stebbins, *ibid.* **55**, 7368 (1997).
  - [5] J. M. Kovac *et al.*, *Nature*, **420**, 772 (2002).
  - [6] A. Kogut *et al.*, *Astrophys. J. Suppl.* **148**, 161 (2003).
  - [7] P. T. Timbie, J. O. Gundersen, and B. G. Keating, in *AMiBA 2001: High-z Clusters, Missing Baryons, and CMB Polarization*, edited by L.-W. Chen *et al.*, ASP Conference Series Vol. 257 (Astronomical Society of the Pacific, San Francisco, CA, 2002); J. E. Carlstrom *et al.*, *Proceedings of "The Cosmic Microwave Background and its Polarization"*, *New Astronomy Reviews*, edited by S. Hanany and K. A. Olive (Elsevier), astro-ph/0308478.
  - [8] C. Burigana *et al.*, *Astron. Astrophys. Suppl.* **130**, 551 (1998).
  - [9] J. H. P. Wu *et al.*, *Astrophys. J. Suppl.* **132**, 1 (2001).
  - [10] L.-Y. Chiang *et al.*, *Astron. Astrophys.* **392**, 369 (2002); R. Vio *et al.*, astro-ph/0309145.

- [11] M. Tristram *et al.*, Phys. Rev. D **69**, 123008 (2004).
- [12] K.-W. Ng and G.-C. Liu, Int. J. Mod. Phys. D **8**, 61 (1999).
- [13] A. Challinor *et al.*, Phys. Rev. D **62**, 123002 (2000); B. D. Wandelt and K. M. Górski, Phys. Rev. D **63**, 123002 (2001).
- [14] T. Souradeep and B. Ratra, Astrophys. J. **560**, 28 (2001).
- [15] P. Fosalba, O. Doré, and F. R. Bouchet, Phys. Rev. D **65**, 063003 (2002).
- [16] E. Newman and R. Penrose, J. Math. Phys. **7**, 863 (1966); J. N. Goldberg *et al.*, *ibid.* **8**, 2155 (1967).
- [17] See, for example, D. A. Varshalovich, A. N. Moskalev, and V. K. Khersonskii, *Quantum Theory of Angular Momentum* (World Scientific, Singapore, 1988).
- [18] I. S. Gradshteyn and I. M. Ryzhik, *Table of Integrals, Series, and Products* (Academic Press, San Diego, 2000).
- [19] A. D. Challinor *et al.*, Mon. Not. R. Astron. Soc. **331**, 994 (2002).
- [20] C.-G. Park *et al.*, Astrophys. J. **589**, 67 (2003).
- [21] M. P. Hobson, A. N. Lasenby, and M. Jones, Mon. Not. R. Astron. Soc. **275**, 863 (1995).
- [22] C.-G. Park and K.-W. Ng, Astrophys. J. **609**, 15 (2004).
- [23] K.-W. Ng, Phys. Rev. D **63**, 123001 (2001).
- [24] A. R. Thompson, J. M. Moran, and G. W. Swenson, *Interferometry and Synthesis in Radio Astronomy* (Wiley, New York, 1986).
- [25] In Ref. [16], the sign  $(-1)^{s+m}$  is absent. We have added the sign in order to match the conventional definition for  $Y_{lm} = {}_0Y_{lm}$ .
- [26] We have corrected the sign errors in the results found in Ref. [12], where  $\alpha \rightarrow -\alpha$  and  $\gamma \rightarrow -\gamma$  should be made in Eqs. (4.6)-(4.9), (6.3), and (9.2).